Fluid Mixing with a Pipeline Tee: Theory and Experiment

The pipeline mixing of two fluid streams by turbulent jet injection normal to the pipeline has been studied theoretically and experimentally. A simple scaling law for the second moment of the tracer concentration within the pipeline is proposed for the first fifteen pipe diameters downstream from the injection point. The similarity solution is derived by assuming that the tracer diffuses in a weak compound jet moving parallel to the pipeline axis. The theoretical results are correlated with all of the available experimental measurements. The results indicate that the second moment of the tracer concentration decreases with increasing jet momentum and distance from the injection point such that $M = 0.25 \cdot (l_m/D)^{-2} (x/D)^{-4/3}$.

L. M. Sroka
L. J. Forney
School of Chemical Engineering
Georgia Institute of Technology
Atlanta, GA 30332

Introduction

Turbulence promotes most important chemical reactions, heat transfer operations, and mixing and combustion processes in industry. Effective use of turbulence increases reactant contact and decreases reaction times, which can significantly reduce the cost of producing many chemicals. Efficient mixing is necessary to obtain profitable yields or to eliminate excessive corrosion in reactor or combustion chambers.

If the necessary contact time between fluids is short, it is common in many existing chemical process units to continuously mix two fluids in a pipeline with subsequent transport to other locations. Although the continuous mixing of two fluid streams can be achieved using a number of mixer geometries, many procedures such as the use of baffles or complex internal geometries will introduce excessive pressure drops and significantly increase the cost of the mixing device. An effective, simple method to mix two fluids within a pipeline is to introduce feed jets such that jet contact with pipeline walls is minimized and mixing occurs rapidly within the turbulent core of the pipeline.

Frequently, a pipeline mixer must be designed for a special processing requirement. Examples of such requirements include the rapid mixing of a small fluid stream into a pipeline of limited length such that flashing or the formation of undesirable products is avoided. Other requirements may be a desired degree of uniformity of the mixture for a specified mixing ratio or mixer geometries that minimize corrosion, scaling or thermal shock to the walls. Additional information is available in the reviews of pipeline mixing with tees and other geometries prepared by Simpson (1974), Gray (1986), and Forney (1986).

The first systematic study of pipeline mixing by jet injection was conducted by Chilton and Genereaux (1930), who used smoke visualization techniques to determine optimum mixing conditions at a glass tee. They concluded that right-angle configurations were effective for good mixing. Chilton and Genereaux also found that when the ratio of the velocity of secondary-to-main flow was in the range of 2 to 3, satisfactory mixing was obtained in 2 to 3 pipeline diameters. Narayan (1971) and Reed and Narayan (1979) used quantitative methods to measure the degree of mixing of air-carbon dioxide feed streams in three pipeline mixers. Narayan, like Chilton and Genereaux, found it was possible to achieve quality mixing in a few diameters with perpendicualr jet injection devices but that parallel flow geometries required up to 250 pipeline diameters.

More recently, Forney et al. (1979, 1982, 1985), Winter (1977), and Maruyama et al. (1981, 1982, 1983) studied the jet injection of fluid into a pipeline over the first twelve pipe diameters from the injection point. Ger and Holley (1976) and Fitzgerald and Holley (1981) compared standard deviations of measured tracer concentrations far downstream (7–120 pipe diameters) from the side tee. Although the objective of the above mentioned research, in both the near and far field, was to establish optimum conditions for pipeline mixing, the experimental data were limited and the results were inconclusive. Typically, the standard deviation or second moment of the tracer concentration was observed to decrease with increasing jet mo-

Correspondence concerning this paper should be addressed to L. J. Forney.

mentum at a fixed measurement point downstream. However, it was difficult to establish a distinct minimum in the second moment of the tracer concentration distribution with increasing jet momentum, particularly within the first twenty pipe diameters from the injection point.

For example, some of the data suggested that impaction of the jet against the opposite wall was necessary to optimize mixing over short distances downstream from the injection point (Maruyama et al., 1981). Other experiments either failed to demonstrate a distinct minimum in the recorded second moment of the tracer concentration or the range of operating conditions was limited (Fitzgerald and Holley, 1981). The mixing criteria used in many of the experiments assumed that optimum mixing in a pipeline was achieved if the jet was centered along the pipeline axis (Forney et al., 1979, 1982, 1985). Although these conclusions are correct for certain values of jet-to-pipe diameter ratio or distance to mix, clearly additional experimental data would be useful to characterize the quality of mixing downstream from a pipeline tee.

Theory

In the present study, fully developed turbulent flow is assumed in both the jet and pipeline. In order to predict the quality of mixing within the pipeline downstream from the injection point, we hypothesize that the mixing of the tracer is controlled by the turbulent characteristics of the jet for several pipe diameters. Moreover, after the initial penetration of the jet into the pipeline, we assume that the jet is moving roughly parallel to the centerline. [In fact, the jet trajectory describes a ⅓ power law with distance downstream (Hoult and Weil, 1972; Wright, 1977).] Farther downstream, however, the mixing of the tracer is influenced solely by the turbulent properties of a fully developed pipeline flow.

Second moment

One useful method of characterizing the uniformity of the mixture within the pipeline is to calculate the second moment of the tracer concentration across the pipeline (Gray, 1986). Thus, we define a second moment in the form

$$M = \frac{1}{A}\int_A \left(\frac{c-\bar{c}}{\bar{c}}\right)^2 dA \tag{1}$$

where the mean concentration is

$$\bar{c} = \frac{1}{A}\int_A c\, dA = c_o\left(\frac{q}{q+Q}\right). \tag{2}$$

Where

A = cross-sectional area of pipeline

c_o = concentration of tracer at the jet inlet

q, Q = injected fluid and initial pipeline volume flow rates

It is also useful to define the initial value of the second moment M_o over the cross section of the main and branch pipes before mixing (Maruyama et al., 1982). Thus, one obtains a value for M as $(x/D) \to 0$ in the form

$$M_o = \frac{\left(\frac{Q}{q}\right)^2\left(\frac{d}{D}\right)^2 + 1}{\frac{d^2}{D^2} + 1}. \tag{3}$$

A dimensional analysis of the problem of right angle jet injection into a pipeline as shown in the schematic of Figure 1 suggests that

$$M = M\left(\frac{l_m}{D}, \frac{x}{D}\right) \tag{4}$$

provided the jet Reynolds number is sufficiently large and the ratio of jet-to-pipe diameter is small (Forney, 1986).

Here, $l_m = (du_o/u_1)$ is the jet momentum length or distance the jet penetrates into the pipeline before it bends over in the crossflow (Hoult et al., 1969; Wright, 1977) and x is the distance downstream from the injection point. It is of interest to note that the initial value of the second moment equals the inverse of the ratio of jet-to-pipeline momentum or $M_o \simeq (l_m/D)^{-2}$ in Eq. 3 since $(l_m/D) = (qD/Qd)$ and $(l_m/D) \ll 1$ for many common jet injection configurations.

Similarity solution

We now seek a similarity solution for the properties of a ducted compound circular jet in the near field as suggested by the work of Curtet and Ricou (1964). Thus, for the tracer concentration profile we assume

$$\frac{c}{c_m} = f\left(\frac{r}{\lambda}\right) = f(\eta) \tag{5}$$

where $c_m = c_m(x)$ is a characteristic maximum jet centerline concentration as indicated in the schematic of Figure 1 and λ is a length scale equal to the width of the jet. It is also assumed that the velocity distribution viewed with respect to the ambient flow is similar or

$$\frac{u-u_1}{u_m-u_1} = \frac{u-u_1}{\Delta u} = g(\eta) \tag{6}$$

where $u_m = u_m(x)$ is the maximum velocity along the jet center-

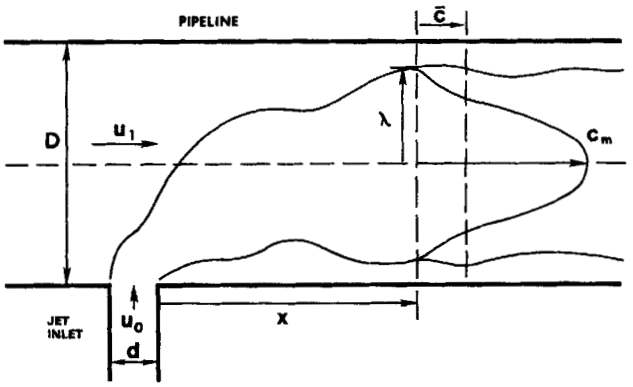

Figure 1. Concentration profile.

line and u_1 is the bulk mean, time-averaged fluid velocity outside the jet.

To simplify the analysis, we now obtain the integral expressions for the conservation of mass, momentum and tracer within a nonbuoyant jet. Since a jet in a crossflow dilutes rapidly in the first pipeline diameter from the injection point as it bends over in the crossflow (Wright, 1977), the analysis below is restricted to the case of a weak jet with $\Delta u/u_1 \ll 1$. Here, $\Delta u = (u_m - u_1)$ is the excess jet velocity above the ambient stream value.

We now write the integral equation for the conservation of mass within the jet of the form

$$\frac{d}{dx}\int_0^\lambda \rho u 2\pi r\, dr = \alpha 2\pi\lambda\rho(u_m - u_1) \tag{7}$$

where α and ρ are constant. Equation 7 introduces an entrainment hypothesis which says that the rate of increase of mass along the jet axis is proportional to the local circumference of the jet times the velocity scale Δu (Hoult et al., 1969; Morton et al., 1956; Rajaratnam, 1976). Assuming a constant density ρ, substituting from Eq. 6 and neglecting terms on the left side of order $\Delta u/u_1$, one obtains

mass: $$\frac{d}{dx}(\lambda^2)\int_0^1 \eta\, d\eta = \frac{\alpha\lambda\Delta u}{u_1}. \tag{8}$$

We now write the integral equation for the conservation of momentum within the jet of the form

$$\frac{d}{dx}\int_0^\lambda \rho u^2 2\pi r\, dr = u_1\frac{d}{dx}\int_0^\lambda \rho u 2\pi r\, dr. \tag{9}$$

Equation 9 says that the rate of change of momentum along the jet is equal to the product of the ambient velocity times the rate of increase of mass. Substituting Eq. 6 and neglecting terms on the order of $(\Delta u/u_1)^2$, one obtains

momentum: $$\frac{d}{dx}(\lambda^2\Delta u)\int_0^1 g(\eta)\eta\, d\eta = 0. \tag{10}$$

Finally, we write the integral equation for the conservation of tracer in the form

$$\frac{d}{dx}\int_0^\lambda cu 2\pi r\, dr = 0. \tag{11}$$

Substituting Eqs. 5 and 6, one obtains

tracer: $$\frac{d}{dx}(\lambda^2 c_m)\int_0^1 f(\eta)\eta\, d\eta = 0. \tag{12}$$

Consistent with the assumption of a self-preserving jet (Rajaratnam, 1976), we now assume that $\lambda \alpha x^q$, $\Delta u \alpha x^p$ and $c_m \alpha x^r$ in Eqs. 8, 10 and 12. Thus, $q = 1/3$, $p = r = -2/3$ and we obtain scaling laws for a weak jet downstream from the injection point of the form

$$\lambda \alpha x^{1/3}, \quad \Delta u \alpha x^{-2/3} \quad \text{and} \quad c_m \alpha x^{-2/3} \tag{13}$$

for the characteristic length, velocity and concentration.

Scaling law for second moment

The definition of the second moment of the tracer concentration within the pipeline can be rewritten in the form

$$M = \left(\frac{c_m^2}{\bar{c}^2}\right)\frac{1}{A}\int_A \left(\frac{c-\bar{c}}{c_m}\right)^2 dA \tag{14}$$

where the definite integral is

$$\frac{1}{A}\int_A \left(\frac{c-\bar{c}}{c_m}\right)^2 dA = \frac{\overline{c^2}-\bar{c}^2}{c_m^2}. \tag{15}$$

It is now useful to relate the maximum concentration c_m in the jet to the mean pipeline value $\bar{c}$. The conservation of tracer becomes

$$\int_0^\lambda cu 2\pi r\, dr = \pi R^2 \bar{c} u_1 \tag{16}$$

where R is the pipeline radius. Therefore, with the substitution of Eqs. 5 and 6, and neglecting terms in the integral on the order of $\Delta u/u_1$, one obtains

$$(c_m\lambda^2)\left[2\int_0^1 f(\eta)\eta\, d\eta\right] = R^2\bar{c}. \tag{17}$$

It is convenient here to define the definite integral in Eq. 17 as

$$\phi_1 = 2\int_0^1 f(\eta)\eta\, d\eta. \tag{18}$$

Substituting Eq. 18 into Eq. 17, one now obtains an expression for the ratio of the mean-to-maximum tracer concentration at a given pipeline cross section of the form

$$\frac{\bar{c}}{c_m} = \phi_1\frac{\lambda^2}{R^2}. \tag{19}$$

In addition, the ratio of the mean square tracer concentration $\overline{c^2}$ to the square of the maximum c_m^2 with the substitution of Eq. 5 becomes

$$\frac{\overline{c^2}}{c_m^2} = \frac{1}{A}\int_A \left(\frac{c}{c_m}\right)^2 dA = \frac{\lambda^2}{R^2}\left[2\int_0^1 f^2(\eta)\eta\, d\eta\right]. \tag{20}$$

It is convenient here to define the definite integral in Eq. 20 as

$$\phi_2 = 2\int_0^1 f^2(\eta)\eta\, d\eta. \tag{21}$$

It is interesting to note that the definite integral of Eq. 15 represents the ratio of the variance of the tracer concentration c at a given pipeline cross section to the square of the maximum value c_m within the jet. Clearly, both the variance of c and the maximum tracer concentration c_m decrease as the jet moves downstream since $\overline{c^2} \to \bar{c}^2$ and $c_m \to \bar{c}$ as $x \to \infty$.

Substituting Eqs. 15, 19 and 20 into Eq. 14, one obtains an expression for the second moment of the tracer concentration in the form

$$M = \frac{R^4}{\phi_1^2\lambda^4}\left[\frac{\lambda^2}{R^2}\phi_2 - \phi_1^2\frac{\lambda^4}{R^4}\right] \tag{22}$$

where the term in brackets represents the ratio of the variance of the tracer concentration c at a given pipeline cross section to the square of its maximum as given by Eq. 15. If we now define the jet-to-pipe area ratio $X = (\lambda^2/R^2)$, the second moment of the tracer concentration can be written in the simple form

$$M = \frac{1}{X^2}\left[X\left(\frac{\phi_2}{\phi_1^2}\right) - X^2\right] \tag{23}$$

or

$$M = \left(\frac{\phi_2}{\phi_1^2}\right)\left(\frac{1}{X}\right) - 1. \tag{24}$$

A circular jet develops a kidney shaped cross section after it is deflected by the cross flow (Rajaratnam, 1976). Since the ratio of the length-to-width of the tracer concentration profile varies from 1.0 to 2.5 as the jet moves downstream, although the velocity distribution remains self-similar (Prattle and Baines, 1967; Keffer and Baines, 1963), it is difficult to specify a simple concentration profile as suggested by Eq. 5. However, it is useful to approximate the concentration distribution as circular in shape with either a gaussian or uniform profile (Schlichting, 1979). Although the actual shape of the profile is not important in the present analysis, the square of the length scale characterizing the width of the jet λ must be proportional to the square of the local mass within the jet divided by its momentum (Forney and Oakes, 1984).

The definite integrals ϕ_1, ϕ_2 and the corresponding second moment M are computed in Table 1 for two approximate concentration distributions. It is now instructive to focus on the functional forms for the second moment M in Table 1. Choosing the uniform or top hat profile for convenience, Eq. 23 suggests that a useful approximation to the second moment M is of the form

$$M = \frac{1}{X} - 1 = \frac{1}{4X^2} + O\left(X - \frac{1}{2}\right)^2 \tag{25}$$

over the important range of the jet-to-pipe area ratio $0.2 < X < 0.7$ as indicated in Figure 2. This result is obtained by expanding

Table 1. Second Moment for Two Distribution Functions where $X = (\lambda^2/R^2)$ and $\eta = (r/\lambda)$

	Schlichting (1979)	Uniform
$\eta \le 1$	$f(\eta) = (1 - \eta^{3/2})^2$	$f(\eta) = 1$
$\eta > 1$	$f(\eta) = 0$	$f(\eta) = 0$
ϕ_1	0.257	1
ϕ_2	0.134	1
ϕ_2/ϕ_1	0.521	1
M	$\frac{2.03}{X} - 1$	$\frac{1}{X} - 1$

$\phi_1 = 2\int_0^1 f(\eta)\eta\, d\eta$

$\phi_2 = 2\int_0^1 f^2(\eta)\eta\, d\eta$

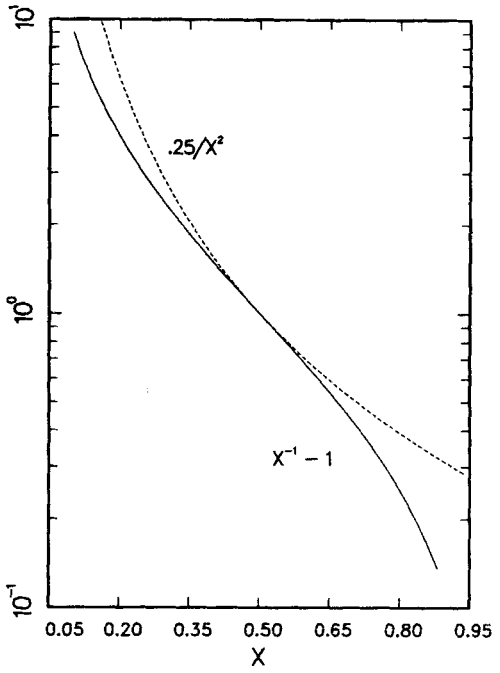

Figure 2. Approximation to second moment for a uniform concentration profile.

both functions of X in Eq. 25 about the point $X = \frac{1}{2}$, or

$$\frac{1}{X} - 1 = 1 - 4\left(X - \frac{1}{2}\right) + 8\left(X - \frac{1}{2}\right)^2 + 0\left(X - \frac{1}{2}\right)^3$$

and

$$\frac{1}{4X^2} = 1 - 4\left(X - \frac{1}{2}\right) + 12\left(X - \frac{1}{2}\right)^2 + 0\left(X - \frac{1}{2}\right)^3.$$

This indicates that the magnitude and slope of the approximate expression for the second moment of the tracer concentration $M \simeq 0.25\, X^{-2}$ is equal to the exact value near the jet-to-pipe area ratio $X = \frac{1}{2}$. This result also implies that the ratio of the variance of the tracer concentration across the pipeline to the square of the maximum concentration defined by the definite integral of Eq. 15 is approximately constant as the jet moves downstream from the injection point.

Since we anticipate that the magnitude of the second moment M may be small or $M \ll 1$ for some conditions within the pipeline, we find it convenient to use the approximation $M \alpha (1/X^2)$ in Eq. 25. Thus, substituting the $\frac{1}{3}$ power law for the length scale λ in Eq. 13 and normalizing with the pipeline diameter D, one obtains a scaling law for the second moment of the tracer concentration of the form

$$M \alpha \left(\frac{x}{D}\right)^{-4/3}.$$

Assuming now that $M \to M_i$ for $(x/D) \to 1$, the second moment of the tracer concentration becomes

$$M = M_i\left(\frac{x}{D}\right)^{-4/3}. \tag{26}$$

Second moment in the far field

Far downstream from the injection point, once the jet has dissipated, the mixing of the tracer is dominated by the fully developed turbulent properties within the pipeline. The concentration distribution for an axisymmetric source in a fully developed turbulent flow was obtained by Jordon (1961) and others from the differential equation for the conservation of the tracer by the separation of variables method.

If the source is axisymmetric, Ger and Holley (1976) used the results of Jordan to determine an approximate expression for the second moment of concentration at large distances from the injection point of the form

$$M = \left[\frac{\phi_3}{J_o^4(\alpha_1)}\right] \exp\left[-1.47\ \sqrt{f}\left(\frac{x}{D}\right)\right] \tag{27}$$

where the definite integral

$$\phi_3 = 2\int_0^1 J_o^2(\alpha_1, \zeta)\zeta\, d\zeta, \tag{28}$$

and

$$\zeta = \frac{r}{R}.$$

Here, f is the pipeline friction factor and α_1 is the first root of the Bessel function $J_o'(\alpha_1) = 0$. Rewriting Eq. 27, one obtains

$$M = 0.157 \exp\left[-1.47\ \sqrt{f}\left(\frac{x}{D}\right)\right]. \tag{29}$$

Ger and Holley generalized the expression for the second moment of the tracer concentration to include asymmetric sources. For an asymmetric source, the constants in Eq. 29 were written in the form

$$M = M_i \exp\left[-k\ \sqrt{f}\left(\frac{x}{D}\right)\right] \tag{30}$$

where $k = 0.46$ for a wall source. Equations 29 and 30 were assumed to be valid provided $(x/D) > (3/\sqrt{f})$ or $(x/D) > 18$ for the pipeline Reynolds number $Re > 20{,}000$ where the friction factor $f = 0.204/Re^{0.208}$.

Experimental Apparatus and Procedures

Apparatus

A schematic of the experimental apparatus is shown in Figure 3. The inlet portion of the primary pipeline was 4 in. schedule 40 PVC pipeline with an inside diameter (ID) of 10.1 cm. The sample section was 10.1 cm ID Lucite tubing. The primary airflow through the pipeline was maintained with a Dayton [12.5 in. (31.8 cm), 1.0 hp (0.75 kW)] blower, downstream from the test section. The total length between the pipeline entrance and the jet injection point was 50 times the pipeline diameter. This ensured that the mainstream flow was fully developed. The blower was capable of producing average pipeline velocities from 6 to 12.5 m/s with corresponding Reynolds numbers from 4×10^4 to 1.2×10^5. Air speed was controlled by restricting flow at the pipeline entrance with screens.

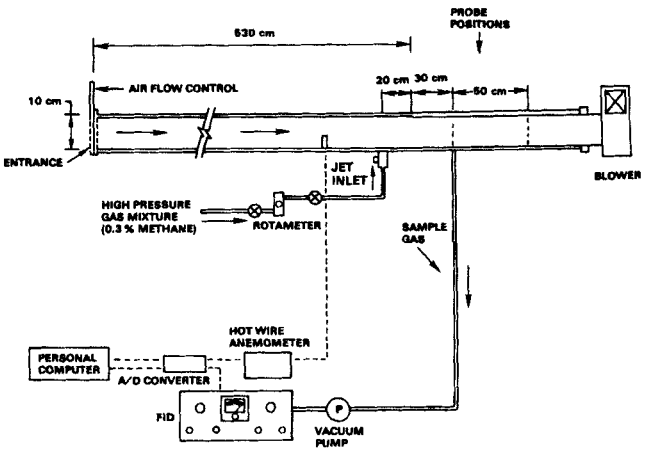

Figure 3. Experimental apparatus.

Jet diameters were varied by using one of several Lucite and glass capillary inserts with inside diameters ranging from 0.07 to 0.95 cm. Jet velocities ranged from 1.5 to 135 m/s and the jet Reynolds numbers ranged from 1×10^3 to 2.2×10^4. A mixture of 0.3% methane, balance air was used as the secondary flow. Jet flow was controlled with a pressure regulator and measured by in-line rotameters. All gases were assumed to be incompressible fluids at the operating conditions of the experiment. Jets were aligned normal to and flush with the pipeline wall. Distances were measured along the pipeline centerline. Measurements could be taken 2, 5 and 10 pipeline diameters downstream from the jet injection point.

Mainstream air velocities were measured with a hot wire anemometer, TSI model 1610 Velocity Transducer with temperature compensation. The anemometer was capable of measuring average axial velocities ranging from 3 to 30 m/s (10 to 100 ft/s). A flame ionization detector, Beckman Model 400, was used to measure the methane concentrations. Both instruments delivered a 0 to 5 V DC signal to the analog-to-digital converter. The digital signal was then stored by a personal computer.

Procedure

The pipeline velocity was determined by measuring the maximum velocity at the centerline while maintaining an appropriate flow rate through the jet. The velocity signal was sampled every 0.5 s for 20 s to obtain a time averaged value for the maximum velocity. After the velocity was obtained, the hot wire anemometer was removed from the pipeline to avoid interference between the probe wake and the jet.

Concentration sample locations were chosen on two diameters: one perpendicular to the plane of the jet and one in the plane of the jet. Each diameter contained 10 equally spaced points plus the center. In all, 21 samples were taken representing cross sectional areas ranging from 1.4% to 7.1% of the total. The concentration signal was sampled every 0.5 s. After the signal stabilized, the last 20 samples were averaged to obtain concentration time averages c_i at each location. It was found that the standard deviation of the 20 sampled concentrations was always less than 2% of the mean value c_i. These time averaged concentrations were used to calculate the second moment values. With the grid system described, the error in the sampled average pipeline concentration was found to be within 10% or less than the value determined from the jet and pipeline volume flowrates.

Results and Discussion

Self-similarity

The validity of Eq. 24 depends on the assumption of self-similarity of the concentration profile within the pipeline. Since it is difficult to determine λ, the characteristic width of the diffusing tracer profile, or equivalently X, the relative area of the diffusing turbulent jet, measured values of $c_m/\bar{c}$ are plotted in Figure 4 as a function of $M + 1$. The solid line in Figure 4 was derived by substitution of Eq. 19 into Eq. 22 or

$$M = \left(\frac{\phi_2}{\phi_1}\right)\left(\frac{c_m}{\bar{c}}\right) - 1 \tag{31}$$

with $(\phi_2/\phi_1) = 0.62$. It should be noted that this empirical value of ϕ_2/ϕ_1 is between the calculated values in Table 1 for the assumed limiting profiles. The difficulty in determining the width or relative jet area arises from the irregular shape of the jet cross section and its intermittent turbulent boundary.

Figure 4 indicates that the ratio of the definite intervals ϕ_2/ϕ_1 is a constant over the range of distances $2 \le (x/D) \le 10$ and jet conditions $0.02 \le (l_m/D) \le 0.55$ in the present study. Moreover, the slope of the data in Figure 4 is a positive one as predicted by Eq. 24. Therefore, the assumption is correct that the concentration profile in the near field of a pipeline mixing tee tends toward that of a self-similar weak jet.

Some of the scatter shown in Figure 4 may be attributed to the experimental methods used in obtaining the data. For example, the tracer concentration measurements were taken on a fixed grid for a given pipeline cross section, while the actual concentration maximum was not restricted to a specific grid location. The three data points on the night of Figure 4 which lie significantly above the theory reflect the inability to measure details of the concentration profiles near the injection point.

Second moment dependence on x/D

The second moment of the tracer concentration decreases with $(x/D)^{-4/3}$ as suggested by the similarity solution of Eq. 26. In order to verify the power law, data were selected from both the present study and the published results of Fitzgerald and Holley (1979), Ger and Holley (1976), and Maruyama et al. (1981, 1983). The data in Figure 5 correspond to contours of fixed diameter and momentum ratio which approximately centered the jet in the pipeline (O'Leary and Forney, 1985). It is evident from Figure 5 that the second moment M is proportional to $(x/D)^{-4/3}$ for diffusing jets for which the assumptions in the theory are valid.

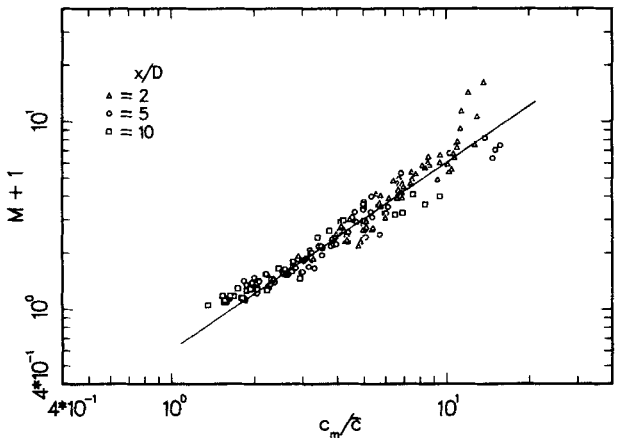

Figure 4. Second moment vs. ratio of maximum-to-mean tracer concentration from the present study for $0.007 < (d/D) < 0.095$.
Solid line is Eq. 31 with $(\phi_2/\phi_1) = 0.62$.

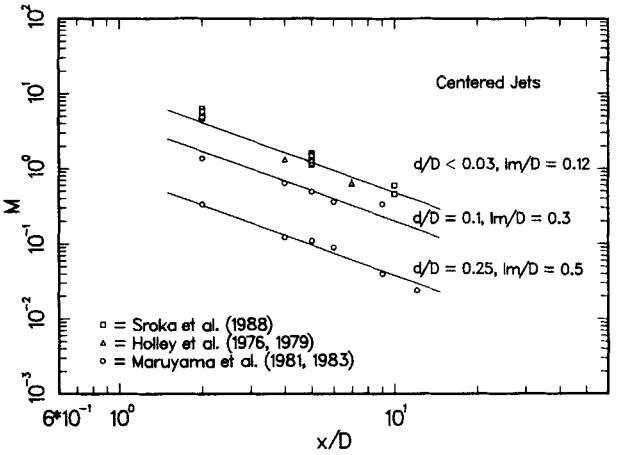

Figure 5. Second moment vs. distance downstream from pipeline tee.

Determination of M_i

The similarity solution has provided the second moment dependence on distance down the pipeline axis. The second moment of the tracer concentration, however, is also a strong function of the ratio of momentum length-to-pipe diameter l_m/D as suggested by experimental data and the dimensional analysis of Eq. 4. In Figure 6 the second moment of the tracer concentration M has been plotted as a function of the jet momentum l_m/D for fixed diameter ratio d/D and distance downstream x/D. As shown in Figure 6, the second moment is independent of momentum ratio for low values such that $(l_m/D) \le 0.07$.

In terms of jet penetration, if $(l_m/D) \le 0.07$ the concentration profiles indicate that the maximum tracer concentration and corresponding jet centerline are near the wall of the pipeline on

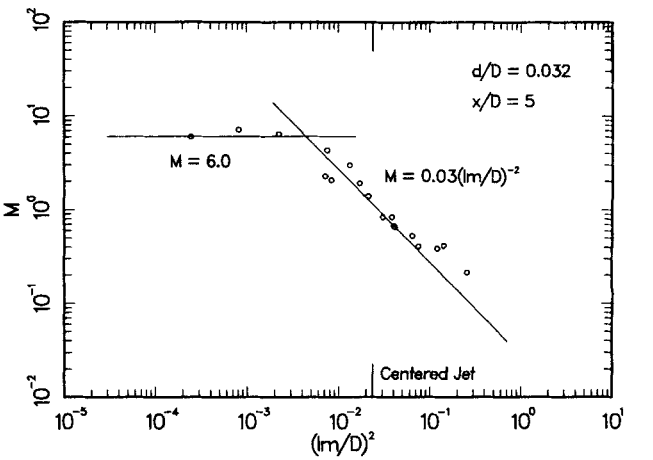

Figure 6. Second moment vs. ratio of jet-to-pipe momentum.

the same side of the jet port. Jets with $(l_m/D) \leq 0.07$ are therefore behaving as a wall source even though the jet has an initial velocity perpendicular to the pipeline axis which differs somewhat from a true wall source.

When the momentum ratio is increased above the wall source value or $(l_m/D) > 0.07$, the second moment of the tracer concentration M can be seen to decrease proportional to $(l_m/D)^{-2}$ in Figure 6. This suggests that the scaling law for the second moment can be written in the form

$$M = k_1 \left(\frac{l_m}{D}\right)^{-2} \left(\frac{x}{D}\right)^{-4/3}. \tag{32}$$

Here, the assumption is made that the initial value $M_i = k_1 (l_m/D)^{-2}$ which corresponds to the limiting value of M as $(x/D) \rightarrow 1$ in Eq. 26. It should also be noted that the form of the boundary condition is suggested by the expression $M_o \simeq (l_m/D)^{-2}$ from Eq. 3, which corresponds to the initial value of the second moment M of the tracer concentration as $(x/D) \rightarrow 0$.

Examination of the tracer concentration profiles corresponding to the intermediate momentum ratios $(l_m/D) > 0.07$ indicates that the location of the maximum tracer concentration penetrates through the crossflow toward the opposite pipeline wall with increasing value of the momentum ratio l_m/D. The lack of a minimum for the second moment of the tracer concentration with increasing l_m/D may be explained since the jet dilution rate is proportional to its rise in the crossflow (Wright, 1977; Hoult and Weil, 1972).

Correlation of second moment data

Figure 7 is a summary of both the new and published experimental data reported as second moment values in the near field of a pipeline mixing tee. The plot demonstrates the effects of the jet-to-pipe momentum ratio and distance downstream from the mixing tee on the second moment of the tracer concentration in a straight pipeline. The diameter ratios represented in Figure 7 range from $0.005 \leq (d/D) \leq 0.255$ over distances downstream from the injection point from $1 \leq (x/D) \leq 12$ in pipeline diameters.

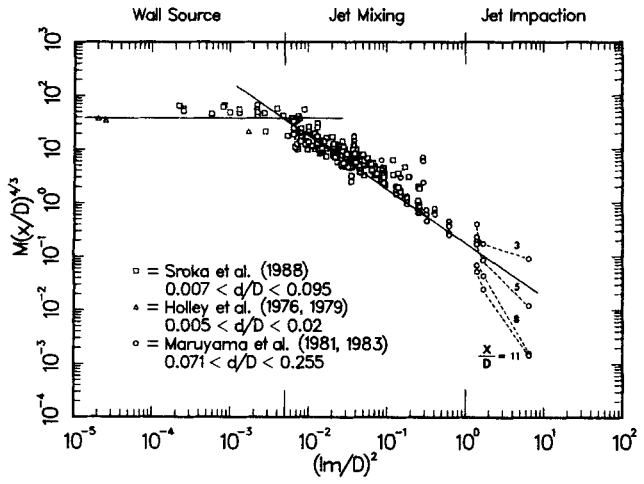

Figure 7. Correlation of second moment in the near field, $(x/D) \leq 12$.
Solid line for jet mixing is Eq. 32 with $k_1 = 0.25$.

Three distinct regions can be noted in Figure 7. As indicated earlier for small values of jet momentum l_m/D, the second moment M is independent of l_m/D and its value corresponds to that of a wall source. In the intermediate range of jet momentum $0.07 \leq (l_m/D) \leq 1.0$, the second moment M decreases with $(l_m/D)^{-2}$ where it was found that the constant $k_1 = 0.25$ in the scaling law of Eq. 32. For $(l_m/D) > 1.0$, the jet impacts with the opposite wall of the pipeline and the dependence of second moment M on the momentum ratio l_m/D is reflected in the data. The dependence of the second moment M on distance downstream from the pipeline tee for both the wall source and the intermediate range of the momentum ratio $(l_m/D) \leq 1.0$ follows the $\frac{4}{3}$ power law as suggested by the similarity solution. For momentum ratios greater than one, however, the $\frac{4}{3}$ power law in x/D is not obeyed. If $(l_m/D) > 1.0$, the slope of the second moment data is greater with increasing jet momentum l_m/D compared to the previous results of Eq. 32.

The secondary effects on the second moment M such as variations in diameter ratio d/D and the jet or pipeline Reynolds number may add to the scatter in the data of Figure 7 but no systematic variation with these groups could be found. Another source of scatter in the plot of Figure 7 is the existence of small minimua in the second moment M in some of the data from Maruyama. These minimua tend to occur at relatively short distances from the injection point for some of the data corresponding to large jet-to-pipe diameter ratios. This indicates that the pipeline walls may be retarding the entrainment of the ambient fluid into the jet for larger diameter ratios d/D.

Second momentum in the far field

For distances greater than fifteen pipeline diameters downstream from the pipe tee, the properties of the jet are no longer self-similar. Figure 8 represents data for values of the second moment of the tracer concentration in the far field $[(x/D) > 17]$ from Ger and Holley (1976) and Fitzgerald and Holley (1979).

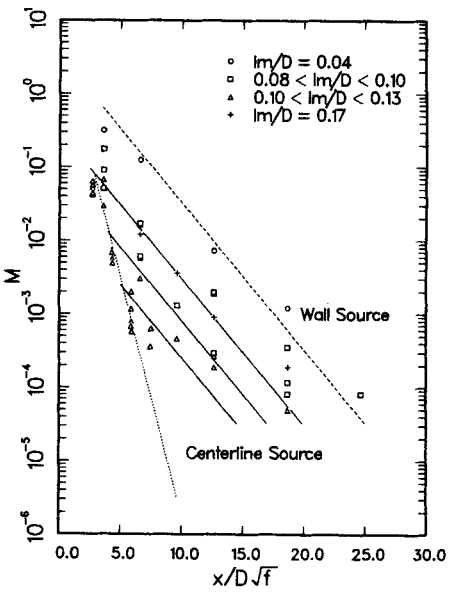

Figure 8. Prediction of second moment in the far field, $(x/D) > 15$.
Dotted line for wall source is Eq. (30) with $M_i = 3.25$ and $k = 0.46$. Solid lines are Eq. 30 with variable M_i. Dashed line for centerline source is Eq. 29.

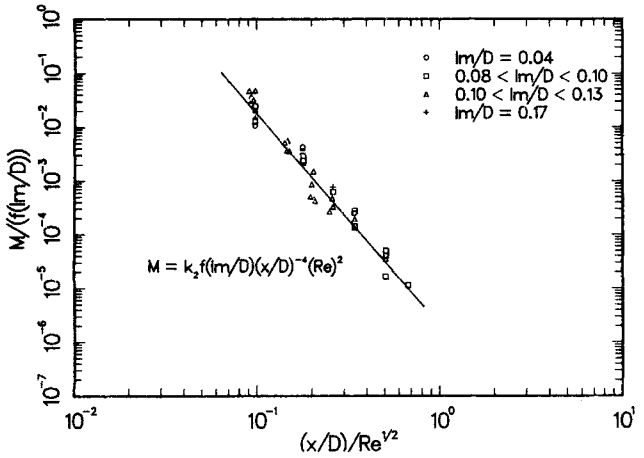

Figure 9. Empirical correlation of far field second moment data.

It is evident from Figure 8 that the second moment of the tracer concentration initially decreases as if the tracer originated from a centerline source as given by Eq. 29. At larger distances downstream from the pipeline tee, however, the second moment decreases with a slope parallel to the wall source of Eq. 30. Here, M_i in Eq. 30 appears to be a function of the ratio of momentum length-to-duct diameter l_m/D.

For the small diameter ratios covering the range $0.005 \le (d/D) < 0.02$ and pipeline Reynolds numbers of $3 \times 10^4 \le Re \le 6 \times 10^4$ in the experiments of Ger and Holley, a minimum in the second moment of the tracer concentration appears to exist for values of $(l_m/D) \simeq 0.12$ as indicated in Figure 8. Thus, it is possible to determine an empirical correlation for the data of Figure 8 in the form

$$M = k_2 f\left(\frac{l_m}{D}\right)\left(\frac{x}{D}\right)^{-4}(Re)^2 \tag{33}$$

where the polynomial is

$$f\left(\frac{l_m}{D}\right) = -0.026\left(\frac{l_m}{D}\right)^{-3} + 1.18\left(\frac{l_m}{D}\right)^{-2} - 14.3\left(\frac{l_m}{D}\right)^{-1} - 53.6. \tag{34}$$

and the constant $k_2 = 1.8 \times 10^{-6}$. The data of Figure 8 are correlated in Figure 9 with Eq. 33.

Acknowledgments

The research was supported in part by a Conoco Graduate Fellowship and a Patricia Roberts Harris Fellowship (L.M.S.). Additional support was provided by the Georgia Institute of Technology Fund (L.J.F.).

Notation

A = area of pipe cross section $(=\pi D^2/4)$, m^2
c = local concentration, mol/m^3
$\bar{c}$ = bulk mean concentration, mol/m^3
c_m = maximum jet centerline concentration, mol/m^3
c_o = tracer concentration at jet inlet, mol/m^3
D = diameter of pipeline, m
d = diameter of jet, m
f = friction factor
$f(\eta)$ = similarity function for concentration profile
$g(\eta)$ = similarity function for velocity distribution
J_o = Bessel function
k = proportionality constant in Eq. 30 (−0.46)
k_1 = proportionality constant in Eq. 32 (−0.25)
k_2 = proportionality constant in Eq. 33 (-1.8×10^{-6})
l_m = jet momentum length (du_o/u_1), m
M = second moment of the tracer concentration
M_i = second moment of the tracer concentration at $(x/D) = 1$
M_o = initial second moment of concentration at $(x/D) = 0$
p, q, r = exponents of similarity variables
Q = volumetric flow rate in pipeline $(=D^2u_1\pi/4)$, m^3/s
q = volumetric flow rate in jet $(=d^2u_o\pi/4)$, m^3/s
r = radial position in pipeline, m
R = radius of pipeline, m
Re = pipeline Reynolds number $[=(\rho u_1 D)/(\mu)]$
u = jet velocity, m/s
u_o = jet velocity at inlet, m/s
u_1 = uniform pipe velocity outside jet, m/s
u_m = maximum jet centerline velocity, m/s
X = ratio of jet-to-pipe cross-sectional area $(=\lambda^2/R^2)$
x = distance downstream from jet, m

Greek letters

α = entrainment coefficient
α_1 = first root of $J_o'(\alpha_1) = 0$
Δu = excess jet velocity $(=u_m - u_1)$
λ = length scale equal to width of jet, m
η = dimensionless length $(=r/\lambda)$
ζ = dimensionless length $(=r/R)$
ϕ_1 = definite integral $(=2\int_0^1 f(\eta)\eta\, d\eta)$
ϕ_2 = definite integral $(=2\int_0^1 f^2(\eta)\eta\, d\eta)$
ϕ_3 = definite integral $(=2\int_0^1 J_0^2(\alpha_1, \zeta)\zeta\, d\zeta)$
ρ = fluid density (k_g/m^3)

Literature Cited

Chilton, T. H., and R. P. Genereaux, "The Mixing of Gases for Reaction," *AIChE Trans.*, **25**, 103 (1930).

Curtet, R., and F. P. Ricou, "On the Tendency to Self-Preservation in Axisymmetric Ducted Jets," *Trans. ASME J. Basic Eng.*, **86**, 765 (1964).

Fitzgerald, S. D., and E. R. Holley, "Jet Injections for Optimum Mixing in Pipe Flow," Research Report No. 144, Water Resources Center, Univ. of Illinois, Urbana, IL (1979).

Fitzgerald, S. D., and E. R. Holley, "Jet Injections for Optimum Mixing in Pipe Flow," *J. Hydraul. Div. ASCE*, **107** (HY 10), 1179 (1981).

Forney, L. J., "Jet Injection for Optimum Pipeline Mixing," *Encylopedia of Fluid Mechanics*, Vol. II, Ch. 25, N. P. Cheremisinoff, ed., Gulf Publishing Co., Houston (1986).

Forney, L. J., and T. C. Kwon, "Efficient Single Jet Mixing in Turbulent Tube Flow," *AIChE J.*, **25**, 623 (July 1979).

Forney, L. J., and H. C. Lee, "Optimum Dimensions for Pipeline Mixing at a T-Junction," *AIChE J.*, **28**(6), 980 (Nov., 1982).

Forney, L. J., and L. A. Oakes, "Slow Second-Order Reactions in a Deflected Buoyant Jet," *AIChE J.*, **30**(1), 30 (Jan., 1984).

Ger, A. M., and E. R. Holley, "Comparison of Single-Point Injections in Pipe Flow," *J. Hydraul. Div. ASCE*, **102**(HY 6), 731 (1976).

Gray, J. B., "Turbulent Radial Mixing in Pipes," *Mixing: Theory and Practice*, Ch. 13, Vol. III, J. B. Gray and V. W. Uhl, eds., Academic Press (1986).

Hoult, D. P., J. A. Fay, and L. J. Forney, "A Theory of Plume Rise Compared with Field Observation," *J. Air Pollut. Cont. Assoc.*, **19**(8), 585 (1969).

Hoult, D. P., and J. C. Weil, "Turbulent Plume in as Laminar Crossflow," *Atmos. Environ.*, **6**, 513 (1972).

Jordan, D. W., "A Theoretical Study of the Diffusion of Tracer Gas in an Airway," *J. of Mech. and Appl. Math*, **14**(2) (1961).

Keffer, J. F., and W. D. Baines, "The Round Turbulent Jet in a Cross-wind," *J. Fluid Mech.*, **15**, 481 (1963).
Maruyama, T., T. Mizushina, and S. Hayashiguchi, "Optimum Jet Mixing in Turbulent Pipe Flow," *Int. Chem. Eng.*, **23**(4), 707 (1983).
Maruyama, T., S. Suzuki, and T. Mizushina, "Pipeline Mixing Between Two Fluid Streams Meeting at a T-Junction," *Int. Chem. Eng.*, **21**(2), 205 (1981).
Maruyama, T., T. Mizushina, and F. Watanabe, "Turbulent Mixing of Two Fluid Streams at an Oblique Branch," *Int. Chem. Eng.*, **22**(2), 287 (1982).
Morton, B. R., G. I. Taylor, and J. S. Turner, "Turbulent Gravitational Convection from Maintained and Instantaneous Sources," *Proc. Roy. Soc. Lond.*, **A234**, (1956).
Narayan, B. C., "Experimental Study of the Rates of Turbulent Mixing in Pipe Flow," M.S. Thesis, Univ. of Tulsa, Tulsa, OK (1971).
O'Leary, C. D., and L. J. Forney, "Optimization of In-Line Mixing at a 90° Tee," *I&EC Proc. Des. & Dev.*, **24**(2), 332 (1985).
Pratte, B. D., and W. D. Baines, "Profiles of the Round Turblent Jet in a Cross Flow," *J. Hydraul. Div. ASCE*, **93**, 53 (1967).
Rajaratnam, N., *Turbulent Jets*, Elsevier Scientific Pub. Co., Amsterdam, Netherlands (1976).
Reed, R. D., and B. C. Narayan, "Mixing Fluids Under Turbulent Flow Conditions," *Chem. Eng.*, 131 (1979).
Schlichting, H., *Boundary Layer Theory*, McGraw-Hill, New York, 7th ed. (1979).
Simpson, L. L., "Turbulence and Industrial Mixing," *Chem. Eng. Prog.*, **70**, 77 (1974).
Winter, D. D., "Turbulent Jet in a Turbulent Pipe Flow," M.S. Thesis, Univ. of Illinois at Urbana–Champaign (1975).
Wright, S. J., "Mean Behavior of Buoyant Jets in a Crossflow," *J. Hydraul. Div. ASCE*, **103**(Hy 5), 499 (1977).

Manuscript received Apr. 12, 1988, and revision received Sept. 20, 1988.